



Formation of abrasion-resistant coatings of the $\text{AlSiFe}_x\text{Mn}_y$ intermetallic compound type on the AISI 304L alloy

Laura G. Martínez-Perales[✉], Alfredo Flores-Valdés, Armando Salinas-Rodríguez, Rocío M. Ochoa-Palacios, José A. Toscano-Giles, Jesús Torres-Torres

Centro de Investigación y de Estudios Avanzados del IPN, Cinvestav-Unidad Saltillo, Avda. Industria Metalúrgica #1062, Ramos Arizpe, C.P. 25900, Coahuila, México

[✉]Corresponding author: laura.martinez@cinvestav.edu.mx, alfredo.flores@cinvestav.edu.mx

Submitted: 15 April 2015; Accepted: 20 November 2015; Available On-line: 10 February 2016

ABSTRACT: The $\alpha\text{-Al}_9\text{FeMnSi}$ and $\beta\text{-Al}_9\text{FeMn}_2\text{Si}$ intermetallics formed by reactive sintering of Al, Si, Mn, Fe, Cr and Ni powders have been used in AISI 304L steels to enhance microhardness. Processing variables of the reactive sintering treatment were temperature (600, 650, 700, 750 and 800 °C), pressure (5, 10 y 20 MPa) and holding time (3600, 5400 y 7200 seconds). Experimental results show that temperature is the most important variable affecting the substrate/coating formation, while pressure does not appear to have a significant effect. The results show the optimum conditions of the reactive sintering that favor the substrate/coating formation are 800 °C, 20 MPa and 7200 seconds. Under these conditions, the reaction zone between the substrate and coating is more compacted and well-adhered, with a microhardness of 1300 Vickers. The results of SEM and X-Ray diffraction confirmed the formation of $\alpha\text{-Al}_9\text{FeMnSi}$ and $\beta\text{-Al}_9\text{FeMn}_2\text{Si}$ intermetallics in the substrate/coating interface as well as the presence of Cr and Ni, indicating diffusion of these two elements from the substrate to the interface.

KEYWORDS: Aluminides; Intermetallic compounds; Stainless steel; $\alpha\text{-Al}_9\text{FeMnSi}$; $\beta\text{-Al}_9\text{FeMn}_2\text{Si}$

Citation / Cómo citar este artículo: Martínez-Perales, L.G., Flores-Valdés, A., Salinas-Rodríguez, A., Ochoa-Palacios, R.M., Toscano-Giles, J.A., Torres-Torres, J. (2016) "Formation of abrasion-resistant coatings of the $\text{AlSiFe}_x\text{Mn}_y$ intermetallic compound type on the AISI 304L alloy". *Rev. Metal.* 52(1):e061. doi: <http://dx.doi.org/10.3989/revmetalm.061>.

RESUMEN: *Formación de recubrimientos resistentes a la abrasión de compuestos intermetálicos del tipo $\text{AlSiFe}_x\text{Mn}_y$ sobre la aleación AISI 304L.* Los intermetálicos $\alpha\text{-Al}_9\text{FeMnSi}$ y $\beta\text{-Al}_9\text{FeMn}_2\text{Si}$ formados por sinterización reactiva de polvos Al, Si, Mn, Fe, Cr, Ni se han utilizado en aceros AISI 304L para mejorar la microdureza. Las variables de procesamiento de sinterización reactiva fueron temperatura (600, 650, 700, 750, y 800 °C), presión (5, 10 y 20 MPa) y el tiempo de retención (3600, 5400 7200 segundos). Los resultados experimentales muestran que la temperatura es la variable más importante que afecta a la formación del sustrato/recubrimiento, mientras que la presión no parece tener un efecto significativo una influencia significativa. Los resultados muestran las condiciones óptimas de la sinterización reactiva que favorecen la formación del sustrato/recubrimiento a 800 °C, 20 MPa y 7200 segundos. En estas condiciones, la zona de reacción entre el sustrato y el recubrimiento es más compacta y bien adherida, con microdureza de 1300 Vickers. Los resultados de MEB y DRX confirman la formación de intermetálicos $\alpha\text{-Al}_9\text{FeMnSi}$ y $\beta\text{-Al}_9\text{FeMn}_2\text{Si}$ en la interfase sustrato/recubrimiento, así como la presencia de Cr y Ni, indicando la difusión de estos dos elementos del sustrato a la interfaz.

PALABRAS CLAVE: Acero inoxidable; Aluminuros; Compuestos intermetálicos; $\alpha\text{-Al}_9\text{FeMnSi}$; $\beta\text{-Al}_9\text{FeMn}_2\text{Si}$

Copyright: © 2016 CSIC. This is an open-access article distributed under the terms of the Creative Commons Attribution-Non Commercial (by-nc) Spain 3.0 License.

1. INTRODUCTION

The use of coatings on various substrates has been a common practice for many years to improve the substrate's resistance to abrasion and/or corrosion, as well as to improve its surface finish and/or appearance. Several applications of coatings include their use on the surfaces of metallic parts in the hottest areas of gas-turbine engines (Clarke *et al.*, 2012) and tubes for heat exchangers. Coatings have also been demonstrated to improve the high-temperature oxidation resistance of plain steel (Das *et al.*, 2004; Mohapatra *et al.*, 2007; Mohapatra *et al.*, 2008). Moreover, it is well-known that different types of alloys, including zinc, transition metal carbides, binary intermetallic compounds, ternary- or multi-constituted alloys, ceramics, etc., have been coated with various materials for improving their resistance to wear and corrosion.

The use of intermetallic compounds has emerged as an important alternative, given the high hardness and high thermal stability that many of these compounds pose. Common intermetallic compounds used today are Al_2Ti , Al_3Ti , Al_3Fe , AlNi_3 , FeCrAlY , TiC , TiN and Cr_{23}C_6 (Sikka *et al.*, 1993; Benci *et al.*, 1995; Li *et al.*, 1997; Han and Xing, 1997; Sun *et al.*, 2009; Dai *et al.*, 2012; Khina and Kulak, 2013; Deng *et al.*, 2014). The aluminides generally are applied on steel surfaces for applications in the electric power industry, petrochemical industry and other energy conversion systems due to their low cost and excellent performance (Kobayashi and Yakou, 2002; Chang *et al.*, 2006; Wang and Chen, 2006).

Two important aspects in the development of high-quality coatings for the above purposes are the uniformity of the protective film over the entire surface area of the substrate and the adhesion between materials. The latter refers to achieving excellent binding of the coating to the base metal. Excellent binding between the base metal and the coating is essential because, under conditions of high friction or chemical attack by corrosive materials, any gap between materials could cause severe leakage during work.

Due to the desire for coatings that demonstrate high hardness values, high thermal stability and excellent adhesion to Fe-based substrates, the idea arose for directly synthesizing $\text{AlSiFe}_x\text{Mn}_y$ -type intermetallic compounds using high-purity powder mixtures for coating purposes. This approach was based on the fact that the elements on the substrates, including Fe, Cr and Ni as well as the intermetallic compounds of Si, Fe and Mn, can diffuse into the substrate, forming a region known as the interdiffusion area (Flores *et al.*, 1999). This interdiffusion area contains sites in which Fe and/or Mn can be exchanged within the crystal structure, both within the substrate itself and in the intermetallic coating, thus obtaining coatings with excellent adhesion to the substrate. However, as described in previous

work (Toscano *et al.*, 2003), the reactive sintering of powders occurs at temperatures greater than 700 °C. In addition, little is known about the kinetics of the phase formation involving, for example, $\alpha\text{-Al}_9\text{FeMnSi}$ and $\beta\text{-Al}_9\text{FeMn}_2\text{Si}$, or the effects on the physical and mechanical properties of the substrate.

In other studies by Orozco *et al.* (2011) characterized quaternary intermetallic phases in Al-Fe-Mn-Si alloys for automotive use in which it worked with proportions of Fe/Mn from 0.1 to 8.4. This study shows that Al-13.4Si-1.1Mn-Fe with ratio by weight Fe/Mn less than or equal to 4, the α -phase presents cubic crystal structure, while in alloys with Fe/Mn equal or greater than 5.3, the α -phase has a hexagonal crystal structure. Therefore, the critical relation Fe/Mn for the transition of crystal structure of cubic to hexagonal transition is it lies between 4 and 5.3 for alloys studied.

Therefore, this study evaluates the influence of the temperature, applied pressure, and sintering time over the thickness, chemical composition and hardness of the coating interface/substrate. In this study, AISI 304L stainless steel was used as the substrate, and the pressures employed ranged up to 20 MPa at temperatures from 600 to 800 °C at holding times of 3600, 5400 and 7200 seconds.

2. EXPERIMENTAL METHODS AND MATERIALS

To prepare the substrates, 304L stainless steel was first cut into 5 mm thick, 1.5 cm×1.5 cm square plates. The surface of the plates was then activated mechanically by blasting with 0.3 mm diameter silica sand. Subsequently, 5 g of an elemental powder mixture of Al, Si, Fe, and Mn was compacted on the activated surface of the substrate using a maximum pressure of up to 5 MPa, producing a powder layer approximately 50 μm thick. The stoichiometric ratio of the powder mixture matched that of the $\alpha\text{-Al}_9\text{FeMnSi}$ intermetallic phase. The plates were then placed in an oven for high-temperature heating using radiation lamps. Each plate was fixed to a universal testing machine that was being used in the compression mode. Compression was performed using two bars of the molybdenum TZM alloy. Argon, supplied at a flow of 0.13 l s⁻¹, was used to create a protective atmosphere. K type thermocouples were placed on the substrates in contact with the powder mixture to detect the thermal events that occur during the coating formation via reactive sintering. The system was connected to a data acquisition system and a computer for producing real-time plots of temperature against time. The pressures employed were 5, 10 and 20 MPa, at temperatures of 600, 650, 700, 750 and 800 °C, with holding times of 3600, 5400 and 7200 seconds at the treatment temperature.

TABLE 1. Metallurgical characteristics of the substrate material

Substrate	Grain size (µm)	Grain morphology	HV (50 g)	wt.%						
				Cr	Ni	Mo	Mn	Co	Si	C
AISI 304L	15	Equiaxed	289	18.49	8.14	0.06	1.54	0.01	0.42	0.03

Upon the completion of each experiment, the types of compounds formed, the metallurgical characteristics of the coating, the nature of the interface coating/substrate, and the Vickers microhardness values (from the intermetallic compound to a few microns into the substrate) were immediately determined. For the characterization of coatings, the samples were cut transversely in half and one side was prepared metallographically. The coating microstructural features were revealed by placing the samples in 0.5% HF for 2 seconds. The elemental concentration profiles were quantitatively determined using X-ray energy dispersive spectrometry (EDS) in a SEM. Microhardness testing was performed in a Vickers hardness tester, using loads of 50 g, as it will be discussed later.

To obtain the stoichiometry of the quaternary intermetallic compounds formed at the side of the coatings made using reactive sintering, the x-ray diffraction patterns of the previously determined α -Al₉FeMnSi and β -Al₉FeMn₂Si intermetallic phases were used (Toscano, 2002) for comparison purposes.

The data in Table 1 show the metallurgical characteristics of the substrates used for the production of coatings including their average grain size, initial hardness and chemical composition in wt.%, wherein the internal reference was the Fe content.

3. RESULTS AND DISCUSSION

In this section the most important results obtained will be presented and discussed. In this sense, the photomicrographs in Fig. 1 show the typical microstructures obtained from the coatings formed at different temperatures using an applied pressure of 20 MPa for 7200 seconds on 304L stainless steel.

It is clear from Fig. 1a that the reaction zones formed during the sintering of the powder mixture

and also the substrate surface is irregular at the interface, indicating that some type of chemical interaction occurred between the particles of the pure elements and the substrate surface. Figure 1b shows that the coating/substrate interface is still irregular at 700 °C, exhibiting a large amount of inclusions. Because EDS microanalysis revealed that these inclusions were mainly rich in Al, Si and O₂, it can be inferred that these inclusions included Al₂O₃ and SiO₂. The source of the SiO₂ particles was attributed to the silica sand used in the blasting operation for the surface activation of the substrate. The Al₂O₃ particles may have been formed by the chemical reduction of Fe, Mn, or Si oxides present in the powder mixture by aluminum. Inclusions may also have previously existed on the surface of the steel sheet; these particles were then trapped due to the speed at which the interface was formed. Finally, Fig. 1c shows the microstructure of a stainless steel sample processed at 800 °C, showing that the intermetallic coating had been fully developed. However, porosity zones are also apparent in Fig. 1c, which were possibly formed by the presence of a molten phase that occurred during the processing of the samples. The coating/substrate interface is continuous along the contact surface and is wider compared to the interfaces obtained at lower temperatures.

In the manufacturing of coatings “in situ”, the formation of a molten AlSi solution occurs during heating. This molten aluminum-rich phase reacts with particles of Fe and Mn in the powder mixture to form intermediate intermetallic compounds that progressively form a coating over the base metal. However, this molten phase could also chemically reduce the oxide films on the substrate. Subsequently, the growth of the alloy layer and quaternary intermetallic formation in the coating is a function of

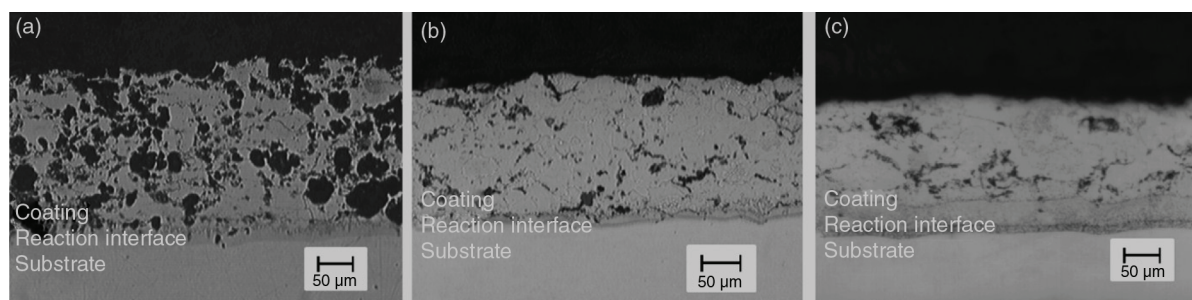


FIGURE 1. Effect of temperature on the formation of surface coating produced on 304L stainless steel by applying a load for over 7200 seconds at 20 MPa: a) 600 °C, b) 700 °C and c) 800 °C.

temperature and processing time. The thickness of the alloy layer depends on the reduction rate of the surface oxide films and on the diffusion speed of the species at the coating layer.

3.1. Influence of pressure and temperature on the interface thickness

The effects of temperature and pressure applied during the reactive sintering of the coating on the interface thickness of the stainless steel substrates are presented in Fig. 2. The effect of the applied pressure on the thickness of the alloy layer is much less important than the effect of temperature on the substrate. Generally, as the temperature and applied pressure increased the thickness of the alloy layer increased as well. This is a consequence of the diffusive nature of the coating formation process, which is favored positively by an increase in temperature and slightly by an increase in the applied pressure. The growth of the interface on the stainless steel alloy exhibits a linear behavior as the temperature increases.

3.2. Scanning electron microscopy in the coatings

The variation in the chemical composition across a slice of the obtained coatings was investigated by EDS microanalysis along a line perpendicular to the interface coating/substrate. The line length was approximately 90 μm and included the coating layer, the alloy layer and the substrate. Analysis was performed to determine the penetration distance of the elements Al, Si, Fe, Mn, Cr, Mo, and Ni into

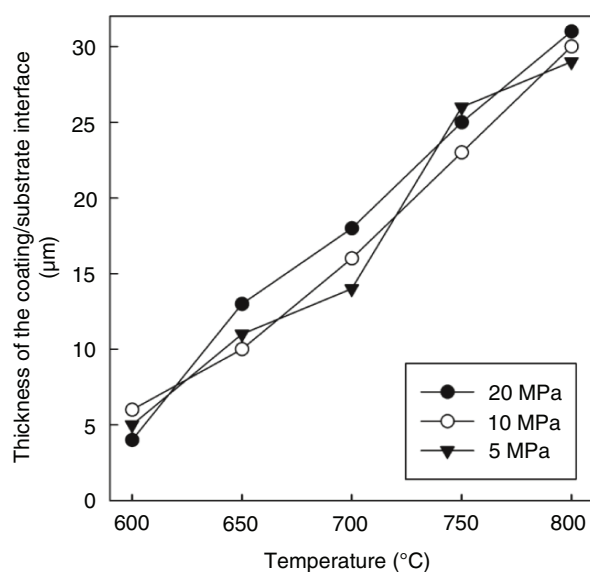


FIGURE 2. Thickness of the coatings obtained as a function of temperature at the pressures indicated after a reaction time of 7200 seconds.

the substrate. Figure 3 shows a SEM micrograph of the microstructure taken with backscattered electrons corresponding to the region where the intermetallic phases co-exists. As it can be seen, there are regions with different average atomic number. Microanalysis by EDS inside these regions showed slight variations in chemical composition. The dark grey phase, marked with the number 1 in Fig. 3 contains 59.27 wt.% Al, 14.25 wt.% Fe, 15.15 wt.% Mn and 11.33 wt.% Si. Meanwhile, the grey phase, identified with the number 2 in the same micrograph, contains 52.26 wt.% Al, 18.40 wt.% Fe, 20.24 wt.% Mn and 9.10 wt.% Si.

According to these results, the phase 1 has the stoichiometric composition $\text{Al}_{8.63}\text{FeMn}_{1.08}\text{Si}_{1.58}$, close to the chemical composition of the intermetallic phase $\alpha\text{-Al}_9\text{FeMnSi}$, while the phase 2 has the average stoichiometric composition $\text{Al}_{7.45}\text{Fe}_{0.5}\text{Mn}_{1.4}\text{Si}_{1.2}$, corresponding to the formula of the $\beta\text{-Al}_9\text{FeMn}_2\text{Si}$ intermetallic.

Figure 4 shows the microanalysis results of a coated stainless steel sample at 600 °C using a pressure of 20 MPa for 7200 seconds; the penetration distances of each element are shown. Under these conditions, no diffusion of any of the elements at the side of the substrate was observed: the composition corresponds solely to that of the stainless steel. Likewise, there is an interface at which all elements are present in both the substrate and the coating. Simultaneously, large variations in the chemical composition are observed, mainly for Al, Si, Fe and Mn. These variations are due to the fact that the quaternary intermetallic compound formed under these conditions is not fully consolidated, and unreacted zones still exist.

Figure 5 shows the concentration profile of a stainless steel sample processed at 800 °C for 7200 seconds at 20 MPa of applied pressure. In addition, this figure shows the presence of all elements in the interface and an even greater penetration of Al and Si into the substrate. On the coating side, the average composition corresponds to the compounds $\alpha\text{-Al}_9\text{FeMnSi}$ and $\beta\text{-Al}_9\text{FeMn}_2\text{Si}$; however, there are also small amounts of Cr and Ni close to the interface regions.

The electron probe mapping of Fig. 6 shows the enrichment of each of the elements according to each area by colors. The Al is observed only in the area of the interface and the coating, while Cr is observed around the substrate, where is concentrated in the area of the interface. The whole area corresponding to the general microstructure is enriched in Fe for more zones of reaction, including the interface and the substrate. Mn also enriches the entire area of the coating and some areas where there are Fe-rich particles. In turn, Mo and Ni concentrate in the area of the interface and the substrate. Nevertheless is observed that molybdenum has spread though the coating and the intermetallic phases.

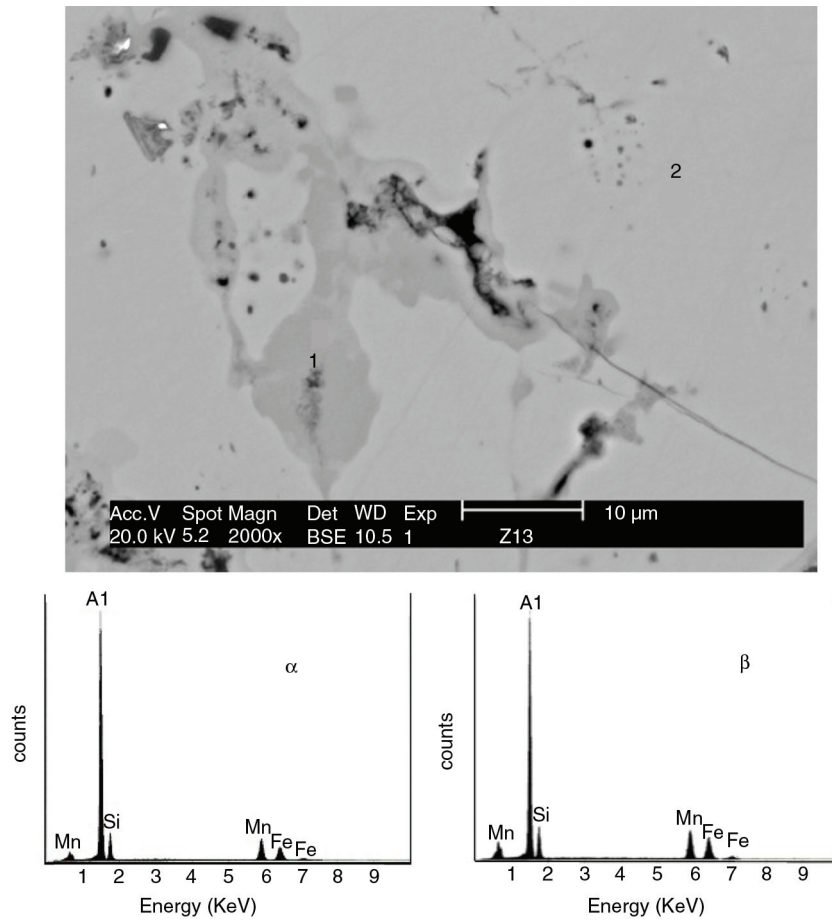


FIGURE 3. Detail of the microstructure of a processed specimen at 800 °C for 7200 seconds by applying a pressure of 20 MPa: 1) 59.27% Al, 14.25% Fe, 15.15% Mn and 11.33% Si; 2) 52.26% Al, 18.40% Fe, 20.24% Mn and 9.10% Si.

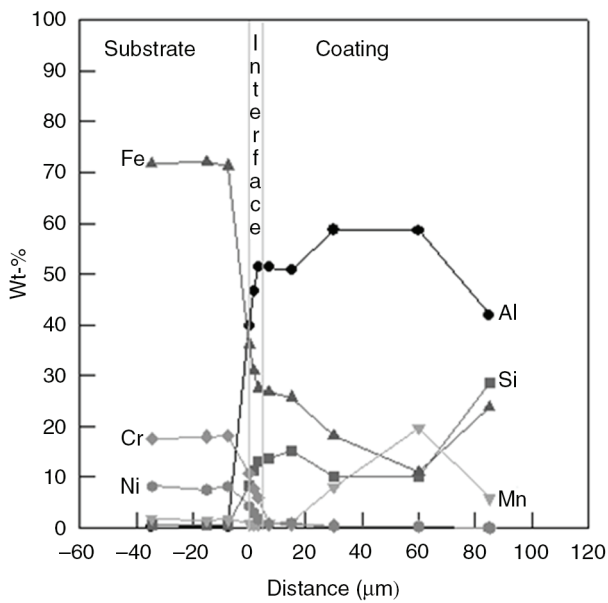


FIGURE 4. Elemental concentration profiles of a coating on 304L stainless steel processed using 600 °C using a pressure of a 20 MPa for 7200 seconds.

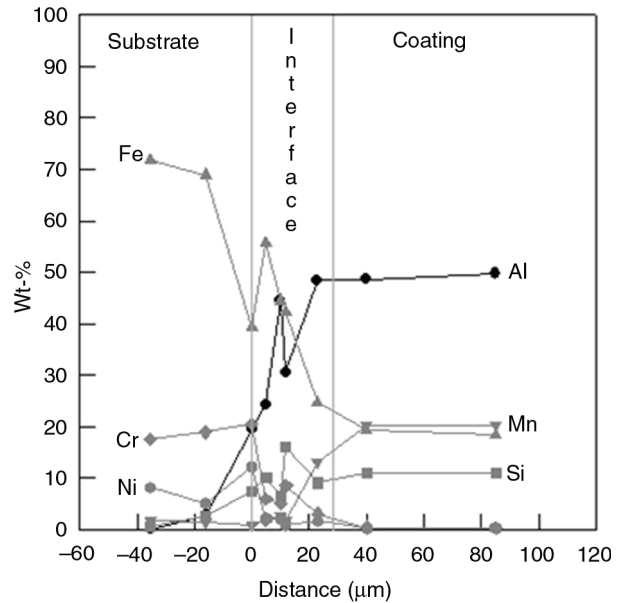


FIGURE 5. Concentration profiles of a coating developed on 304L stainless steel at 800 °C using a pressure of 20 MPa for 7200 seconds.

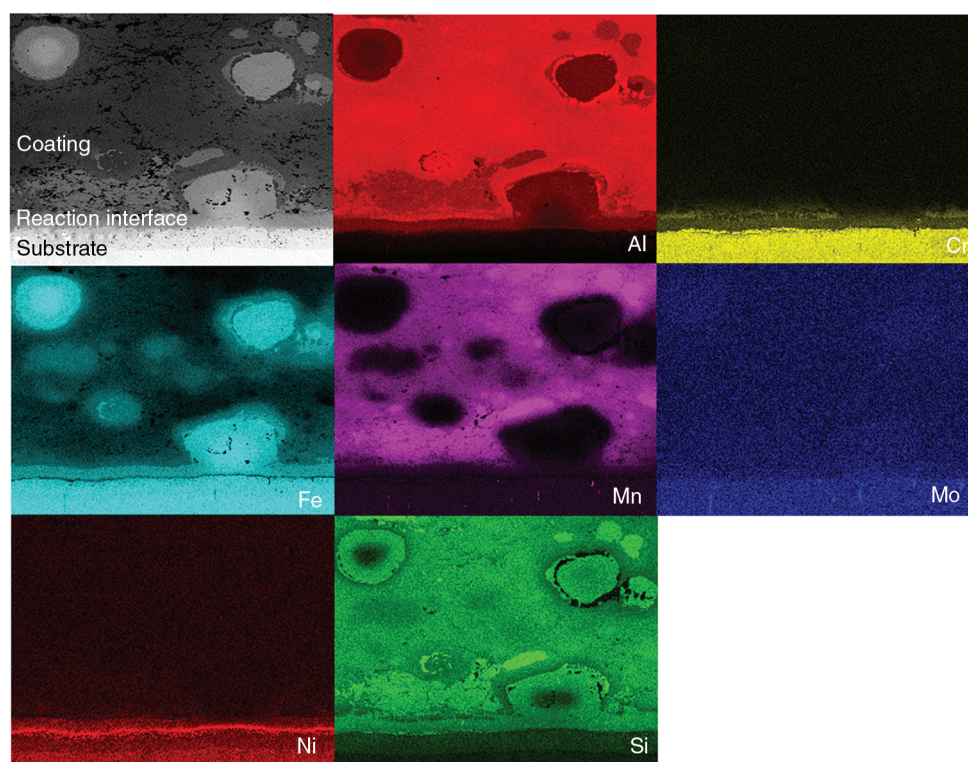


FIGURE 6. General microstructure and elemental maps of a processed specimen at 800 °C, with an application of pressure of 20 MPa for 7200 seconds.

Finally, Si is concentrated inside the interface of reaction but in homogeneous concentration around the intermetallic phases.

Several crystallography studies of iron-rich intermetallics (especially β -phase intermetallics) in Al-alloys have been undertaken since 1981, but it is important to note that commercial Al-Si alloys invariably contain significant amounts of Fe and Mn as well as other elements that affect the stability of quaternary intermetallic phases (Kral *et al.*, 2004).

From these results, it can be established that Al, Si, Fe, Mn, Cr and Ni form a small region of continuity at the coating/substrate interface. This differs slightly from the original proposal, as it was believed that only chromium played an important role in the formation of the interface. Figure 7 shows the diffraction pattern obtained from a coating on stainless steel processed using 800 °C and a load of 20 MPa for 7200 seconds. The peaks in Fig. 7 correspond to the chemical composition of the α -Al₃FeMnSi and β -Al₃FeMn₂Si phases: cubic and hexagonal, respectively.

The above results establish that the formation of coatings by reaction sintering from elemental powders generate various profiles on the stainless 304L steel substrate. Clearly, this behavior is controlled by the physical-chemical characteristics of the base metal surface.

It is important to note that the coatings obtained at 800 °C consist of two quaternary phases with different crystal structures, as stated previously. The SEM images show no structural defects in the coating; thus, the two phases are well coupled and no cracks were generated during the coating process.

3.3. Microhardness

Before presenting the corresponding results to this section, it is important to state that the applied load during microhardness testing is of paramount importance in choosing that to clearly define the microhardness value attained, specifically for such a hard and brittle phases as intermetallic compounds (Borrero-López and Hoffman, 2014). In this sense, Fig. 8 is a composition of photomicrographs and microhardness values of a coating processed at 800 °C, using a pressure of 20 MPa after a reaction time of 7200 seconds. The values were taken at the intermetallic layer hand side. As it can be seen, after applied loads above 20 MPa, the intermetallic phase begins to show striations clearly seen at the borders of each indentation. As of these results, it was decided to perform microhardness measurements using a load of 50 g. Next, Fig. 9 shows the effect of temperature on the microhardness of coatings on

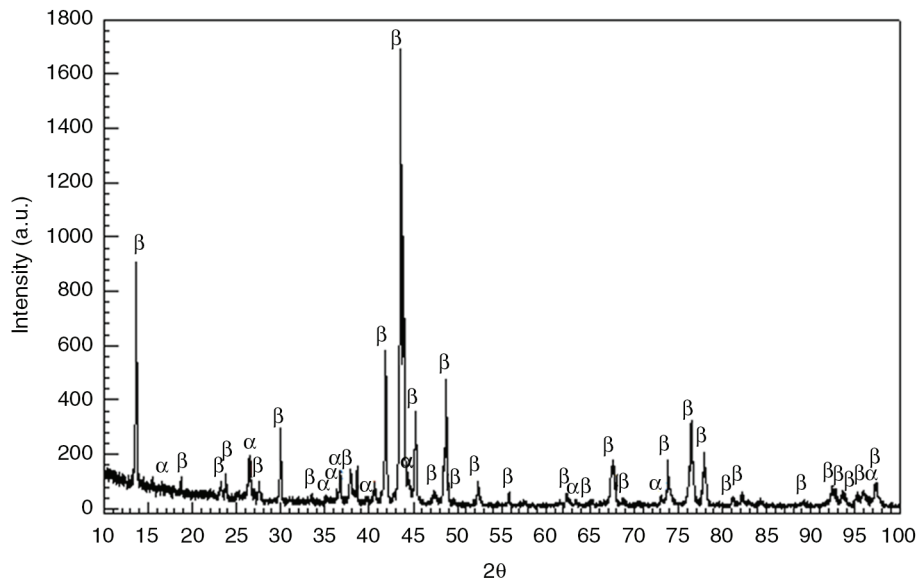


FIGURE 7. Diffraction pattern obtained from a coating on 304L stainless steel at 800 °C under an applied pressure of 20 MPa for 7200 seconds.

304L stainless steel after 7200 seconds of processing at the indicated pressures. As noted, the coating exhibits low microhardness values, on the order of 1000 kg mm^{-2} , at temperatures below 700 °C. These low values are because the coating does not completely form under these conditions, and there are several phases in this microstructure lowering the hardness values. As shown previously, the increase in temperature during the formation of the coating causes an increase in hardness of the coating and the coating/substrate interface, achieving hardness values of 1065 and 1300 kg mm^{-2} , respectively. The effect of the applied pressure is also shown; however, as previously discussed, its effect is less than that of temperature.

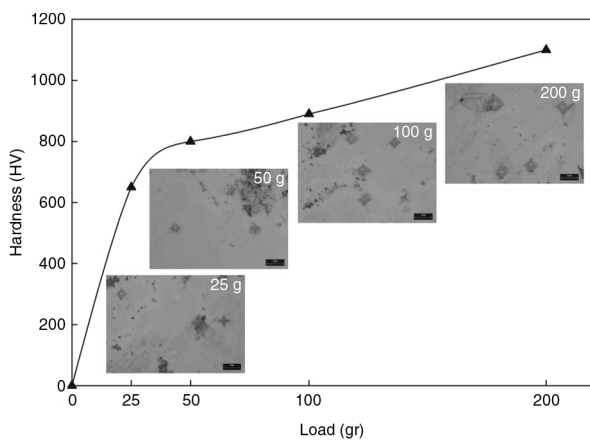


FIGURE 8. Microhardness values as a function of applied load on the intermetallic layer side of a coating formed at 800 °C, using a pressure of 20 MPa after a reaction time of 200 seconds.

In addition, Fig. 9 demonstrates that the hardness of the substrate is not influenced by the pressure nor by the processing temperature, which exhibits a value of 290 kg mm^{-2} . This value is similar to the value determined for the substrate before applying the coating (289 kg mm^{-2}). This result indicates that the substrate does not change its microstructure during the reactive sintering process.

According to the results obtained during this stage of the work, it is noted that the best coatings

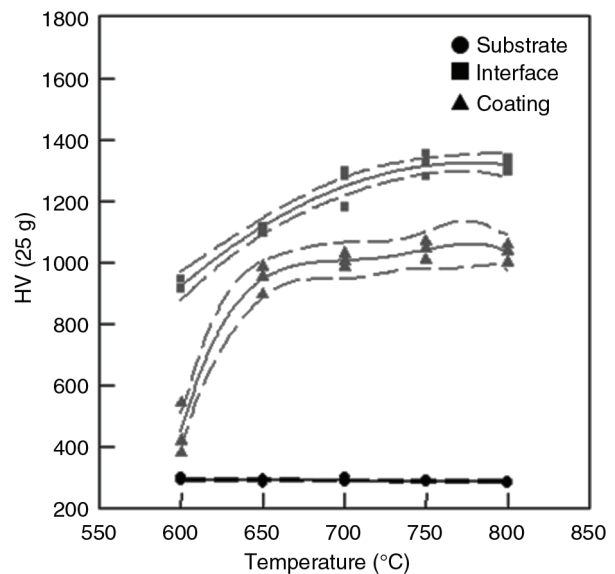


FIGURE 9. Microhardness values of coatings on 304L stainless steel as a function of temperature for the indicated pressure and 7200 seconds of reaction.

were obtained at 20 MPa of applied pressure for 7200 seconds while holding at 800 °C. The interface generated in these cases was continuously interlocked with the base material, achieving high hardness values due to the incorporation of Cr and/or Ni into the structure.

3.4. Kinetic study

Figure 10 shows a fragment of the recorded curve in a coating processed at 800 °C on a 304L stainless steel substrate using an applied pressure of 5 MPa for 3600 seconds. As shown in Fig. 10, the temperature of the sample initially increases linearly with time until it reaches approximately 580 °C. At 580 °C, the slope decreases but the temperature continues to rise at a slower rate until 610 °C is reached. In this temperature range, the heating rate registered was 0.25 °C s^{-1} , which is less than the predetermined heating rate in the furnace controller (0.8 °C s^{-1}). This observation indicates that the sample absorbs heat from the surroundings, which can be associated with the melting of a solid Al-Si solution formed by solid state diffusion during the heating of the powder mixture. Therefore, it can be concluded that this process also occurs during the formation of the coatings. Figure 10 also shows that after 610 °C, the slope of the curve increases suddenly to a value of 4.3 °C s^{-1} , indicating the release of heat in the system. This event can be attributed to the chemical reaction between the molten Al-Si phase with Fe and/or Mn to form intermediate ternary phases, which was observed in a previous study (Whittenberger, 1990). The y axis at the right hand side of the curve corresponds to the first derivative dT/dt . The first derivative shows that at the onset of the coating formation, the temperature reaches

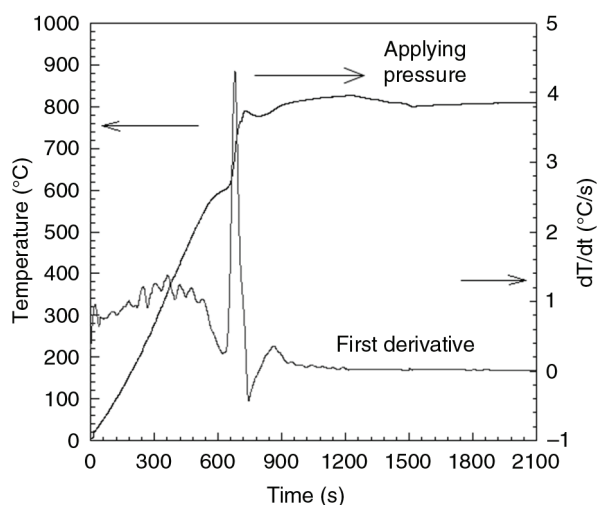


FIGURE 10. Temperature-time data and the first derivative curve recorded during the formation of a coating onto 304L stainless steel at an applied pressure of 5 MPa for 2100 seconds.

as high as 880 °C. This observation provides an idea of how much heat is released during the reactive sintering processing of the coatings onto the stainless steel surface.

Once the temperature reached 800 °C at constant pressure, it was no longer possible to detect significant changes in the system temperature. Figure 11 shows the complete set of experimental measurements about the total amount, in % in area, of the $\alpha\text{-Al}_9\text{FeMnSi}$ and $\beta\text{-Al}_9\text{FeMn}_2\text{Si}$ intermetallic compounds formed as a function of holding time, at the constant pressure of 20 MPa.

Nevertheless, the formation and growth of the intermetallic-substrate interface can be explained as follows. During heating, the interface is formed by solid state diffusion in an Al-Si solution, which melts at approximately 579 °C. Then, this molten phase immediately reacts with Fe and/or Mn at the substrate surface. As the time, temperature and pressure increase, the rate of diffusion of the chemical species from the substrate surface and from the coating to the interface controls the coating thickness obtained. During the coating preparation while using a constant applied pressure, the intermetallic phase formation starts at approximately 600 °C.

Whittenberger (1990) performed an analysis of the solid state diffusion through a layer of reaction products around particles of pure elements. The described mechanism of the formation of the intermetallic compounds was based on the assumption that the interfacial reactions were not limiting but depended mainly on the solid state diffusion through the intermediate microstructures formed once reactive sintering had been initiated. In this sense, the equations reported by Whittenberger (1990) could be used to determine the values of several kinetic parameters that determine the reaction rate of the $\text{AlSiFe}_x\text{Mn}_y$ intermetallic compound formation.

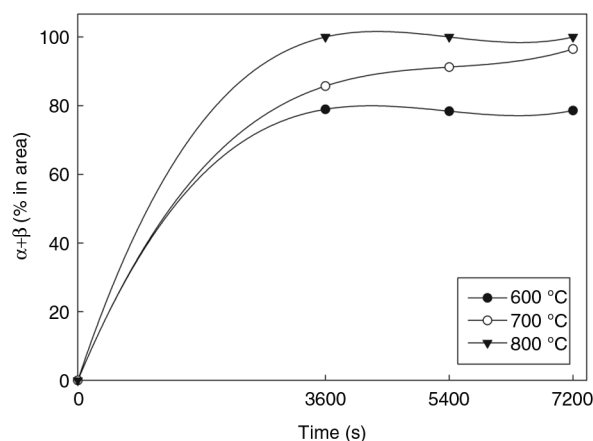


FIGURE 11. Total amount, in % area, of the $\alpha\text{-Al}_9\text{FeMnSi}$ and $\beta\text{-Al}_9\text{FeMn}_2\text{Si}$ intermetallic compounds formed as a function of holding time for the temperatures indicated, at an applied pressure of 20 MPa.

The distance over which diffusion occurs is proportional to the square root of the product of the diffusion coefficient of volume D_v and the time t :

$$d \propto \sqrt{D_v t} \quad (1)$$

If it is assumed that the growth of the intermetallic diffusion can be approximated by the unidirectional diffusion coefficient, which is independent of concentration, Eq. (1) can be represented as:

$$D_v = z^2 / 64t \quad (2)$$

where z represents the distance between the nucleus/intermetallic and intermetallic/nucleus contiguous interfaces and can be equal to the particle size.

For a diffusion time of 3600 seconds and where z equals 3.27×10^{-3} cm for an iron-rich nucleus, the value of D_v^{Fe} obtained is equal to 4.64×10^{-11} cm² s⁻¹. For a time of 3600 seconds and where z equals 2.64×10^{-3} cm for a manganese-rich nucleus, the value of D_v^{Mn} obtained is equal to 3.02×10^{-11} cm² s⁻¹. Once the value of D_v is determined, the activation energy of the process can be calculated using the Arrhenius equation, which is described as:

$$D_v = A \exp(-Q/RT) \quad (3)$$

where A is a constant representing the frequency factor (cm² s⁻¹), Q the activation energy (kJ mol⁻¹), R the universal gas constant (kJ mol⁻¹ K⁻¹), and T the absolute temperature (K).

Considering that if, for Mn-rich nucleus, $D_v = 3.02 \times 10^{-11}$ cm² s⁻¹, $A = 104$ cm² s⁻¹, $R = 8.31 \times 10^{-3}$ kJ mol⁻¹ K⁻¹ and $T = 873$ K, the Eq. (3) yields a value of Q equal to 209 kJ mol⁻¹. This value is consistent with the value reported in the literature for the diffusion of Mn in Al, i.e., 211.4 kJ mol⁻¹.

For Fe-rich nucleus, $D_v = 4.64 \times 10^{-11}$ cm² s⁻¹, $A = 135$ cm² s⁻¹, $R = 8.31 \times 10^{-3}$ kJ mol⁻¹ K⁻¹ and $T = 873$ K, for which a value of Q equal to 208 kJ mol⁻¹ is obtained. This value is also close to that reported in the literature for the diffusion of Fe in Al, which is 192.6 kJ mol⁻¹. According to the calculated values and the activation energy for the diffusion coefficients of Fe and Mn in aluminum, the speed at which these species diffuse through the layer of products is very similar. However, these values are merely an approximation and may not accurately represent the speed with which diffusion occurs due to the unknown nature of the intermediate products formed during reactive sintering.

4. CONCLUSIONS

According to the results obtained in this work, it can be concluded that the best conditions for obtaining surface coatings of α -Al₉FeMnSi and β -Al₉FeMn₂Si on the surface of 304L stainless steel by reactive

sintering from elemental powders include a temperature of 800 °C, an applied pressure of 20 MPa and 7200 seconds of holding time. Under these conditions, the interface generated is well-adhered to the substrate, reaching hardness values on the order of 1300 Vickers. The coating has an excellent adherence to the surface due to the interdiffusion of elements from the intermetallics and of Cr and/or Ni from the substrate that form a reaction zone rich in Al, Fe, Mn, Si, Cr and Ni, approximately 36 μ m thick. The mechanism of the intermetallic formation is diffusive, in which the diffusion of Fe and Mn through the Al is the controlling step. However, it is believed that the formation of an AlSi molten state during the process aided in accelerating the process.

ACKNOWLEDGEMENTS

The authors wish to thank the Council National of Science and Technology (CONACYT) for the economic support provided, Project CB-822511.

REFERENCES

- Benci, J.E., Ma, J.C., Feist, T.P. (1995). Evaluation of the intermetallic compound Al₂Ti for elevated-temperature applications. *Mat. Sci. Eng. A-Struct.* 192–193, 38–44. [http://dx.doi.org/10.1016/0921-5093\(94\)03201-7](http://dx.doi.org/10.1016/0921-5093(94)03201-7).
- Borrero-López, O., Hoffman, M. (2014). Measurement of fracture strength in brittle thin films. *Surf. Coat. Tech.* 254, 1–10. <http://dx.doi.org/10.1016/j.surfcoat.2014.05.053>.
- Clarke, D.R., Oechsner, M., Padture, N.P. (2012). Thermal-barrier coatings for more efficient gas-turbine engines. *Mat. Res. Soc.* 37 (10), 891–898. <http://dx.doi.org/10.1557/mrs.2012.232>.
- Chang, Y., Tsaur, C.C., Rock, J.C. (2006) Microstructure studies of an aluminide coating on 9Cr-1Mo steel during high temperature oxidation. *Surf. Coat. Tech.* 200 (22–23), 6588–6593. <http://dx.doi.org/10.1016/j.surfcoat.2005.11.038>.
- Dai, Y., Boutellier, V., Gavillet, D., Glasbrenner, H., Weisenburger, A., Wagner, W. (2012) FeCrAlY and TiN coatings on T91 steel after irradiation with 72 MeV protons in flowing LBE. *J. Nucl. Mater.* 431 (1–3), 66–76. <http://dx.doi.org/10.1016/j.jnucmat.2011.11.006>.
- Das, S.K., Joarder, A., Mitra, A. (2004). Magnetic Barkhausen emissions and microstructural degradation study in 1.25 Cr–0.50 Mo steel during high temperature exposure. *NDT&E Int.* 37 (4), 243–248. [http://dx.doi.org/10.1016/S0963-8695\(03\)00032-X](http://dx.doi.org/10.1016/S0963-8695(03)00032-X).
- Deng, B., Tao, Y., Zhu, X., Qin, H. (2014). The oxidation behavior and tribological properties of Si-implanted TiN coating. *Vacuum* 99, 216–224. <http://dx.doi.org/10.1016/j.vacuum.2013.06.006>.
- Flores, A., Castillejos, A., Acosta, A.H., Bocado, F., Toscano, A. (1999). *The Development of Surface Coatings for Co-Cr-Mo alloys Based on Quaternary AlSiFeMn Intermetallic Compounds, Cobalt-Base Alloys for Biomedical Applications*, J.A. Disegi, R.L. Kennedy, R. Pilliar (Eds.), American Society for Testing and Materials, USA, pp. 179–189. <http://dx.doi.org/10.1520/STP14273S>.
- Han, Y.F., Xing, Z.P. (1997). *Structural Intermetallics. Development and Engineering Application of a DS cast Ni₃Al Alloy IC6*, M. Nathal, R. Darolia, C.T. Liu, P.L. Martin (Eds.), Minerals, Metals and Materials Society, USA, pp. 713–719.
- Khina, B.B., Kulak, M.M. (2013). Effect of ultrasound on combustion synthesis of composite material “TiC metal binder”. *J. Alloy Compd.* 578, 595–601. <http://dx.doi.org/10.1016/j.jallcom.2013.07.030>.
- Kobayashi, S., Yakou, T. (2002). Control of intermetallic compound layers at interface between steel and aluminum by

- diffusion-treatment. *Mat. Sci. Eng. A-Struct.* 338 (1–2), 44–53. [http://dx.doi.org/10.1016/S0921-5093\(02\)00053-9](http://dx.doi.org/10.1016/S0921-5093(02)00053-9).
- Kral, M.V., McIntyre, H.R., Smillie, M.J. (2004). Identification of intermetallic phases in a eutectic Al-Si casting alloy electron backscatter diffraction pattern analysis. *Scripta Mater.* 51 (3), 215–219. <http://dx.doi.org/10.1016/j.scriptamat.2004.04.015>.
- Li, S., Zhang, J., Wang, B., Zhang, J., Zou, D., Jia, T., Gong, Z. (1997). *Structural Intermetallics. Study on superplasticity of deformed Ti₃Al and TiAl base alloys*, M.V. Nathal, R. Darolia, C.T. Liu, P.L. Martin (Eds.), Minerals, Metals and Materials Society, USA, pp. 361–367.
- Mohapatra, J.N., Panda, A.K., Gunjan, M.K., Bandyopadhyay, N.R., Mitra, A., Ghosh, R.N. (2007). Ageing behavior study of 5Cr–0.5Mo steel by magnetic Barkhausen emissions and magnetic hysteresis loop techniques. *NDT&E Int.* 40 (2), 173. <http://dx.doi.org/10.1016/j.ndteint.2006.08.001>.
- Mohapatra, J.N., Ray, A.K., Swaminathan, J., Mitra, A. (2008). Creep behaviour study of virgin and service exposed 5Cr–0.5Mo steel using magnetic Barkhausen emissions technique. *J. Magn. Magn. Mater.* 320 (18), 2284–2290. <http://dx.doi.org/10.1016/j.jmmm.2008.04.152>.
- Orozco, P., Castro, M., López, J., Hernández, A., Muñoz, R., Luna, S., Ortiz, C. (2011). Effect of iron addition on the crystal structure of the α -AlFeMnSi phase formed in the quaternary Al-Fe-Mn-Si system. *Rev. Metal.* 47 (6), 453–461. <http://dx.doi.org/10.3989/revmetalm.1068>.
- Sikka, V.K., Viswanathan, S., Mc Kamey, C.G. (1993). *Structural Intermetallics. Development and Commercialization status of Al₃Ti Based Intermetallics Alloy*, R. Darolia, J.J. Lewandowski, C.T. Liu (Eds.), Minerals, Metals and Materials Society, USA, pp. 483–491.
- Sun, R.L., Lei, Y.W., Niu, W. (2009). Laser clad Cr₃C₂-Ni composite coating on titanium alloys. *Surf. Eng.* 25 (3), 206–210. <http://dx.doi.org/10.1179/026708409X375299>.
- Toscano, J.A. (2002). *Procesamiento y Microestructura de Compuestos Intermetálicos Al(FeMn)Si Elaborados Mediante Sinterización Reactiva de Polvos Asistido con Presión Uniaxial*. PhD Thesis, CINVESTAV-IPN, Unidad Saltillo, México, pp. 62–68.
- Toscano, J.A., Flores, A., Salinas, A., Nava, E. (2003). Microstructure of Al₉(Fe,Mn)₃Si intermetallics produced by pressure-assisted reactive sintering of elemental AlMnFeSi powder mixtures. *Mater. Lett.* 57 (15), 2246–2252. [http://dx.doi.org/10.1016/S0167-577X\(02\)01204-1](http://dx.doi.org/10.1016/S0167-577X(02)01204-1).
- Wang, C.J., Chen, S.M. (2006). The high-temperature oxidation behavior of hot-dipping Al-Si coating on low carbon steel. *Surf. Coat. Tech.* 200 (22–23), 6601–6605. <http://dx.doi.org/10.1016/j.surfcoat.2005.11.031>.
- Whittenberger, J.D. (1990). *Solid State Processing for High Temperature Alloys and Composites, Solid State Powder Processing*, A.H. Clauer, J.J. de Barbadillo (Eds.), Minerals, Metals and Materials Society, USA, pp. 137–155.